Photophysical Properties of $CpRe(CO)_2L$ Complexes. Distinct Orbital Emissions from Nonequilibrated Excited States in Room Temperature Solution

Marsha M. Glezen and Alistair J. Lees*

Contribution from the Department of Chemistry, University Center at Binghamton, State University of New York, Binghamton, New York 13901. *Received December 5, 1988*

Abstract: Luminescence spectra obtained from $CpRe(CO)_2L$ complexes [Cp = η^5-C_5H_5 and L = pyridine (py) or 4-phenylpyridine (4-Phpy)] in deoxygenated room temperature solution display three distinct maxima in the visible region. Electronic absorption spectra, emission quantum yields, emission lifetimes, excitation spectra, and low-temperature data have been measured to characterize the nature and dynamics of the participating excited states. In 210–293 K fluid solution the two lowest energy emissions are assigned to thermally equilibrated $^3MLCT(b_2)$ and $^3MLCT(e)$ levels, and the upper energy band originates from a nonequilibrated ^3LF state. At 293 K the ^3MLCT emission lifetime is relatively long-lived ($\tau_e \sim 1$–5 μs) and, contrastingly, the ^3LF emission decay is rapid ($\tau_e < 0.5$ ns). Room-temperature emission is also observed from the closely related $CpRe(CO)_2(pip)$ (pip = piperidine) complex, supporting the ^3LF assignment. Kinetic analysis of the emission data illustrates that the $^3MLCT(b_2)$ and $^3MLCT(e)$ levels can be fitted to a Boltzmann model placing their energy separation at 860 cm^{-1}. A key feature of this photophysical system is that the ^3LF state undergoes much more rapid radiative decay ($k_r > 2.6 \times 10^6$ s^{-1}) than that of the equilibrated ^3MLCT manifold ($k_r = 32$ s^{-1} and 6.6×10^3 s^{-1}). When the solution is cooled to 80 K and forms a frozen glass, the MLCT absorption and emission bands undergo significant blue shifts, and the thermal equilibrium between the ^3MLCT levels is lost. The nonequilibration properties of these $CpRe(CO)_2L$ complexes are discussed on a photophysical model involving a highly distorted $^3MLCT(b_2)$ state.

Photophysical studies are the key to understanding the nature of the lowest electronically excited state present in a molecule. Since it is usually this state which fundamentally determines a molecule's photochemistry, it is necessary from a mechanistic viewpoint to determine what factors are ultimately responsible for its rate of energy deactivation. Luminescent techniques are a very sensitive means by which one can successfully probe excited states and their deactivation pathways.

Our understanding of the emission properties of organometallic complexes is still very limited due to the fact that relatively few species have been established to luminescence, especially in solution at room temperature.[1] The vast majority of metal complexes which do emit exhibit a single emission band and are, therefore, in accordance with Kasha's well-known rule which states that only the lowest energy excited state is luminescent for any given multiplicity.[2] Moreover, in transition-metal compounds extremely efficient intersystem processes are believed to take place, and this generally precludes the observation of emission from their singlet levels.

In recent years much attention has been paid to the luminescence behavior of metal complexes that possess closely spaced low-lying excited states. These proximate excited states can be of very different orbital characters, for instance they may involve metal-centered (MC), charge-transfer (CT), or intraligand (IL) transitions.[1] Indeed, many molecules have been established to display multiple-state emission,[3] and a few systems even exhibit multiple luminescence features in fluid solution.[4] In almost all of these examples the multiple emission in solution has been demonstrated to arise from two thermally equilibrated levels, and the participating excited states have been represented by Boltzmann population models.[4,5] To our knowledge there are only two literature reports at this time that describe nonequilibrated emissions from metal complexes in fluid solution, and in each of these it is fluorescence and phosphorescence features that have been resolved.[6]

Recently, on studying the emission properties of a series of d^6 $CpRe(CO)_2L$ compounds, where Cp = η^5-C_5H_5, and L = pyridine (py), 4-phenylpyridine (4-Phpy), and piperidine (pip), we have discovered an extraordinarily rich and significant photophysical system.[7] The observed photophysical behavior is most unusual

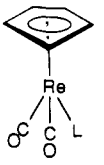

L = py, 4-Phpy, pip

because three distinct luminescence maxima are determined from the pyridine derivatives in both fluid and in frozen solutions; even at room temperature the emitting states are apparently not all thermally equilibrated. Moreover, the photophysics of these complexes are especially noteworthy because distinct orbital emissions are obtained in room-temperature solution. This paper is concerned with a full description of the photophysical data for the $CpRe(CO)_2L$ system, and it presents a model that details the excited-state interconversion processes and relaxation mechanisms.

Experimental Section

Materials. All solvents and materials are commercially available and used without further purification, unless otherwise noted below. Rhenium pentacarbonyl chloride was purified by repeated sublimations under re-

(1) (a) Fleischauer, P. D.; Fleischauer, P. *Chem. Rev.* **1970**, *70*, 199. (b) Wrighton, M. *Chem. Rev.* **1974**, *74*, 401. (c) Geoffroy, G. L.; Wrighton, M. S. *Organometallic Photochemistry*; Academic Press: New York, 1979. (d) Lees, A. J. *Chem. Rev.* **1987**, *87*, 711.

(2) Kasha, M. *Discuss. Faraday Soc.* **1950**, *9*, 14.

(3) (a) For a review of literature appearing up to 1980, see: DeArmond, M. K.; Carlin, C. M. *Coord. Chem. Rev.* **1981**, *36*, 325. (b) Sullivan, B. P.; Abruna, H.; Finklea, H. O.; Salmon, D. J.; Nagle, J. K.; Meyer, T. J.; Sprintschnik, H. *Chem. Phys. Lett.* **1978**, *58*, 389. (c) Rader, R. A.; McMillin, D. R.; Buckner, M. T.; Matthews, T. G.; Casadonte, D. J.; Lengel, R. K.; Whittaker, S. B.; Darmon, L. M.; Lytle, F. E. *J. Am. Chem. Soc.* **1981**, *103*, 5906. (d) Martin, M.; Krogh-Jespersen, M.-B.; Hsu, M.; Tewksbury, J.; Laurent, M.; Viswanath, K.; Patterson, H. *Inorg. Chem.* **1983**, *22*, 647. (e) Belser, P.; von Zelewsky, A.; Juris, A.; Barigelletti, F.; Balzani, V. *Chem. Phys. Lett.* **1984**, *104*, 100. (f) Segers, D. P.; DeArmond, M. K.; Grutsch, P. A.; Kutal, C. *Inorg. Chem.* **1984**, *23*, 2874. (g) Casadonte, D. J.; McMillin, D. R. *J. Am. Chem. Soc.* **1987**, *109*, 331. (h) Blakley, R. L.; DeArmond, M. K. *J. Am. Chem. Soc.* **1987**, *109*, 4895.

(4) (a) Watts, R. J. *Inorg. Chem.* **1981**, *20*, 2302. (b) Kirchhoff, J. R.; Gamache, R. E.; Blaskie, M. W.; Del Paggio, A. A.; Lengel, R. K.; McMillin, D. R. *Inorg. Chem.* **1983**, *22*, 2380. (c) Nishizawa, M.; Suzuki, T. M.; Sprouse, S.; Watts, R. J.; Ford, P. C. *Inorg. Chem.* **1984**, *23*, 1837. (d) Zulu, M. M.; Lees, A. J. *Inorg. Chem.* **1989**, *28*, 85.

(5) Kemp, T. J. *Prog. React. Kinet.* **1980**, *10*, 301.

(6) (a) Kirk, A. D.; Porter, G. B. *J. Phys. Chem.* **1980**, *84*, 887. (b) Sexton, D. A.; Ford, P. C.; Magde, D. *J. Phys. Chem.* **1983**, *87*, 197.

(7) Preliminary results have been communicated, see: Glezen, M. M.; Lees, A. J. *J. Am. Chem. Soc.* **1988**, *110*, 6243.

0002-7863/89/1511-6602$01.50/0

duced pressure. Ligands piperidine (pip) and pyridine (py) were distilled under nitrogen and then chromatographed on a neutral alumina column. The 4-phenylpyridine (4-Phpy) ligand was sublimed repeatedly before use. Tetrahydrofuran (THF) used in the synthetic procedures was distilled from $LiAlH_4$ and stored under an argon atmosphere. The solvent mixture EPA (5:5:2 diethyl ether/isopentane/ethanol) used for low-temperature measurements was prepared from spectral grade solvent components which had been dried and purified according to standard laboratory practices.[8] All solvents used in the emission experiments were rigorously purified to ensure removal of emitting or quenching impurities. Nitrogen used for purging was dried and deoxygenated according to a previously reported procedure.[9]

Synthesis of $CpRe(CO)_3$. This complex was prepared by refluxing rhenium pentacarbonyl chloride (2.0 g) and cyclopentadienylthallium (1.3 g) in hexane (250 mL) for 24 h, analogous to a literature procedure.[10] A resultant white compound was obtained in 82% yield on filtering the reflux mixture and rotary evaporating the solvent. The product was purified by repeated sublimations under reduced pressure: mp 111–112 °C (lit. mp 112 °C);[11] IR $CpRe(CO)_3$ in CCl_4, ν(CO) 2025, 1937 cm^{-1} (lit. in C_8H_{18}, 2028, 1938 cm^{-1}).[12]

Synthesis of $CpRe(CO)_2$(pip). This compound was prepared by direct irradiation (typically for 1 h) with a 200 W mercury arc lamp of a deoxygenated benzene solution (50 mL) containing the parent $CpRe(CO)_3$ complex (10^{-4} M) and excess pip (10^{-2} M), according to a previously reported procedure.[12] The product was obtained on rotary evaporating the solvent. The residue was purified by column chromatography on silica gel; elution with hexane removed unreacted $CpRe(CO)_3$, and subsequent elution with benzene gave the yellow product complex in a 20% yield. The $CpRe(CO)_2$(pip) complex was further purified by recrystallization from a 10:1 hexane/dichloromethane solution. The fairly air-sensitive compound was handled under N_2 and stored in the dark: IR $CpRe(CO)_2$(pip) in CCl_4, ν(CO) 1913, 1839 cm^{-1} (lit. in C_8H_{18}, 1915, 1846 cm^{-1}).[12]

Synthesis of $CpRe(CO)_2L$ (L = py, 4-Phpy). These complexes were obtained via thermal reaction of the appropriate ligand L with the prior photochemically generated THF adduct, $CpRe(CO)_2$(THF), by modification of a previously published method.[12] Typically, a deoxygenated THF solution (50 mL) of $CpRe(CO)_3$ (10^{-4} M) was photolyzed with a 200 W mercury arc lamp for 1 h to produce the THF adduct which was subsequently allowed to react with L for 15 min at room temperature in the dark to form the product. These reaction steps were monitored by UV–vis spectroscopy. The products were then obtained and purified in a similar manner to that described above for the $CpRe(CO)_2$(pip) complex. Following purification the $CpRe(CO)_2L$ compounds were typically obtained in 15–20% yields. The compounds were also prepared by direct photolysis of $CpRe(CO)_3$ in the presence of excess entering ligand. These derivatives were moderately stable as solids and were kept in the dark under N_2 to enhance their long-term stability: IR $CpRe(CO)_2$(py) in CCl_4, ν(CO) 1920, 1851 cm^{-1} (lit. in C_8H_{18} 1921, 1857 cm^{-1});[12] $CpRe(CO)_2$(4-Phpy) in CCl_4, ν(CO) 1920, 1853 (lit. in C_8H_{18} 1925, 1860 cm^{-1}).[12]

Equipment and Procedures. Infrared spectra were obtained from the complexes as solutions using a NaCl cell of 1 mm pathlength; the data were recorded on a Perkin-Elmer 283B spectrometer, and the maxima are considered accurate to ±2 cm^{-1}. Electronic absorption spectra were recorded on a Hewlett-Packard Model 8450A diode-array spectrometer, and the reported band maxima are accurate to ±2 nm. Emission and excitation spectra were obtained on a SLM Instruments Model 8000/8000S spectrometer which incorporates a photomultiplier-based (Hamamatsu R928) photon counting detector. These spectra were fully corrected for variations in detector response and excitation lamp intensity as a function of wavelength, and the band maxima are found to be reproducible to within ±4 nm.

In the emission and excitation experiments the sample solutions were filtered through 0.22 μm Millipore filters and deoxygenated prior to taking measurements. UV–vis and IR spectra were checked before and after irradiation to monitor possible sample degradation. The solution temperature was controlled to ±0.1 K in these emission experiments. Excitation spectra were recorded from samples that were optically dilute ($A < 0.1$) throughout the spectral region scanned. Excellent agreements were obtained between the excitation and absorption spectra for the known standards quinine sulfate and 1,2-benzanthracene under these optically dilute conditions.[13] Emission quantum yields (ϕ_e) were determined at 293 K by using the Parker–Rees method with dilute quinine sulfate in deoxygenated 0.2 M H_2SO_4 ($\phi_e = 0.55$)[14] or dilute $Ru(bpy)_3^{2+}$ in deoxygenated aqueous solution ($\phi_e = 0.042$)[15] as calibrants; the ϕ_e values were corrected for differing refractive indices of the solvents, as reported previously.[16] The emission quantum yields were reproducible to within ±15%.

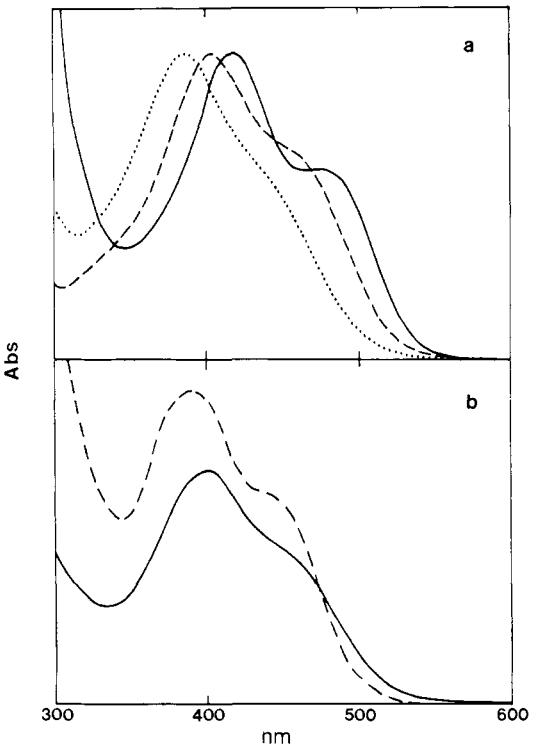

Figure 1. Electronic absorption spectra of $CpRe(CO)_2$(4-Phpy) in (a) methylene chloride (···), benzene (– –), and isooctane (—) at 293 K and in (b) EPA at 80 K (– –) and 293 K (—). The low-temperature spectrum is not corrected for solvent contraction.

Emission lifetimes (τ_e) were recorded on a PRA System 3000 time-correlated pulsed single photon counting apparatus.[17] Samples were excited with light from a PRA Model 510 nitrogen flashlamp that was transmitted via an Instruments SA Inc. H-10 monochromator, and emission was detected at 90° by means of a second H-10 monochromator and a thermoelectrically cooled red-sensitive Hamamatsu R955 photomultiplier tube. The resultant photon counts were stored on a Tracor Northern Model 7200 microprocessor-based multichannel analyzer. The instrument response function was subsequently deconvoluted from the emission data to obtain an undisturbed decay that was fitted by using a least-squares procedure on an IBM PC; the reported errors on the lifetimes represent the reproducibility of readings over at least three measurements.

Low-temperature absorption and emission experiments were undertaken with an Oxford Instruments DN1704K liquid nitrogen cryostat containing a 1-cm pathlength quartz cell. In all of these low-temperature measurements the solution was rigorously deaerated prior to taking readings with a freeze–pump–thaw procedure. The temperature of the solution in the cryostat was maintained to ±0.2 K with an Oxford Instruments Model 3120 controller.

Results

Electronic absorption spectra of the $CpRe(CO)_2L$ (L = py and 4-Phpy) complexes are dominated by two intense (ϵ = 2500–6000 M^{-1} cm^{-1}) broad bands in the visible region. The energy positions of these low-lying transitions are dependent on the solution temperature and the nature of the solvent and py ligand; spectra observed from $CpRe(CO)_2$(4-Phpy) in various room-temperature solutions and in an EPA glass are illustrated in Figure 1. The

(8) Gordon, A. J.; Ford, R. A. *The Chemist's Companion, a Handbook of Practical Data, Techniques, and References*; Wiley: New York, 1972.
(9) Schadt, M. J.; Gresalfi, N. J.; Lees, A. J. *Inorg. Chem.* **1985**, *24*, 2942.
(10) King, R. B.; Reimann, R. H. *Inorg. Chem.* **1976**, *15*, 179.
(11) Fischer, E. O.; Fellman, W. *J. Organomet. Chem.* **1963**, *1*, 191.
(12) Giordano, P. J.; Wrighton, M. S. *Inorg. Chem.* **1977**, *16*, 160.
(13) Berlman, I. B. *Handbook of Fluorescence Spectra of Aromatic Molecules*; 2nd ed.; Academic Press: New York, 1971.
(14) Parker, C. A.; Rees, W. T. *Analyst* **1960**, *85*, 587.
(15) Van Houten, J.; Watts, R. J. *J. Am. Chem. Soc.* **1976**, *98*, 4853.
(16) Demas, J. N.; Crosby, G. A. *J. Phys. Chem.* **1971**, *75*, 991.
(17) O'Connor, D. V.; Phillips, D. *Time-Correlated Single Photon Counting*; Academic: London, 1984.

Table I. Electronic Absorption, Excitation, and Emission Spectral Data for $CpRe(CO)_2L$ Complexes in Deoxygenated Benzene at 293 K and EPA Glasses at 80 K[a]

L	solvent	temp, K	absorption λ_{max}, nm	excitation λ_{max}, nm	emission λ_{max}, nm	emission $\phi_e \times 10^4$	emission τ_e
py	C_6H_6	293	373, 412	*b*	A 420 (sh)[b,c]	*b*	*b*
				340, 360 (sh), 410	B 492	0.12 (±0.018)[e]	1.0 (±0.3) μs
				340, 360 (sh), 410	C 676	0.10 (±0.015)[e]	1.0 (±0.2) μs
	EPA	80	356, 396 (sh)		B 488		7.8 (±0.6) μs
					C 646		12.6 (±0.5) μs
4-Phpy	C_6H_6	293	338 (sh), 404, 448	346	A 440[c]	0.02 (±0.005)[d]	<0.5 ns
				346, 402, 450	B 542	0.47 (±0.07)[e]	4.5 (±0.9) μs
				346, 402, 450	C 710	1.7 (±0.3)[e]	4.5 (±0.4) μs
	EPA	80	386, 435		A 430 (sh)[f]		8.3 (±0.4) μs
					B 512		71 (±10) μs
					C 656		6.5 (±0.2) μs
pip	C_6H_6	293	338	344	A 440[c]	13 (±2)[d]	0.5 (±0.1) ns
	EPA	80	336		A 432		11.5 (±0.3) μs
CO	C_6H_6	293	255		*g*		
	EPA	80	255		*g*		

[a] Excitation and emission spectra are fully corrected for wavelength variations in instrumental response; emission data recorded following excitation at 380 nm unless otherwise noted; lifetimes and excitation data obtained at the corresponding emission maxima. [b] Very weak emission observed; excitation data, quantum yields, and lifetimes not obtained. [c] Excitation at 330 nm. [d] Absolute yield measured relative to 0.55 value for quinine sulfate in 0.2 M H_2SO_4 (see ref 14). [e] Absolute yield measured relative to 0.042 value for $Ru(bpy)_3^{2+}$ in aqueous solution (see ref 15). [f] Excitation at 320 nm. [g] No emission observed.

$CpRe(CO)_2(py)$ complex displays similar features, but the broad absorption band envelope is significantly blue-shifted. In comparison, the $CpRe(CO)_3$ and $CpRe(CO)_2(pip)$ complexes exhibit lowest energy absorption bands in the UV region (see Table I).

Emission spectra of the $CpRe(CO)_2L$ (L = py and 4-Phpy) complexes in room-temperature solution are striking as they each display three distinct features. These emission spectra are reproducible for different preparation and purification methods of the $CpRe(CO)_2L$ complexes, ruling out emission from a common sample or solvent impurity. Emission from a photochemically produced impurity or dimeric species has also been excluded on the evidence that the emission spectral distribution is not affected by varying the irradiation time during which these measurements were taken. For convenience, the three emission features are hereafter denoted as bands A, B, and C, designated in order of their decreasing energy position.

Figure 2 depicts the emission spectrum recorded from $CpRe(CO)_2(4\text{-Phpy})$ in deoxygenated benzene at 293 K; the $CpRe(CO)_2(py)$ complex exhibits a similar spectrum with the two most intense emission bands B and C being somewhat blue-shifted (see Table I). In both complexes the third weak emission band A is centered at 420–440 nm; this band is also observed from the $CpRe(CO)_2(pip)$ derivative at 440 nm (see Figure 2). Emission quantum yields have been obtained from the complexes in 293 K solution; these have been determined for each of the individual emission bands and are summarized in Table I. Significantly, no emission was detected from either the parent $CpRe(CO)_3$ complex or the free ligands themselves following excitation at these wavelengths.

Bands B and C of the 4-Phpy and py complexes were observed to be solvent dependent and exhibit solvent shifts in a parallel direction to those noted in the absorption spectra. For example, excitation at 380 nm of $CpRe(CO)_2(4\text{-Phpy})$ in deoxygenated benzene gave rise to emission band maxima B and C at 542 and 710 nm. When the medium is changed to a CH_2Cl_2 solution, these maxima shift to 504 and 690 nm, respectively. In contrast, the energy position of band A at 440 nm is not significantly affected by this solvent change.

Emission lifetimes obtained from all of the complexes and each of the bands are listed in Table I. A short subnanosecond decay has been recorded from band A at 440 nm of the $CpRe(CO)_2(4\text{-Phpy})$ complex in room-temperature solution. The lifetime observed from the $CpRe(CO)_2(pip)$ complex in 293 K benzene solution is also determined to be very short. Contrastingly, the emission lifetimes of bands B and C from the $CpRe(CO)_2L$ (L = py, 4-Phpy) complexes in 293 K solution are relatively long-lived being in the microsecond region. Importantly, for both the py and 4-Phpy complexes the emission lifetimes are the same from either of the two low-lying emission bands B and C; indeed, this was found to be the case at any fluid solution temperature measured between 210 and 293 K.

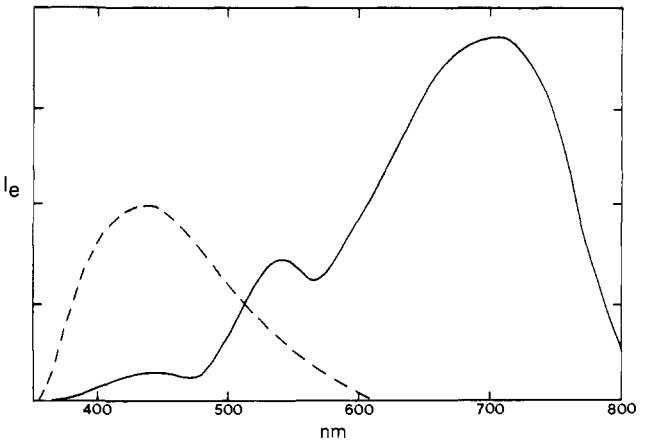

Figure 2. Emission spectra of $CpRe(CO)_2(4\text{-Phpy})$ (—) and $CpRe(CO)_2(pip)$ (– –) in deoxygenated benzene at 293 K. Spectra were recorded following excitation at 330 nm and are corrected for wavelength variations in detector response.

Low-temperature emission data have been obtained from the compounds in frozen EPA glasses at 80 K. Similar emission features A, B, and C were observed from the py or 4-Phpy complexes, although bands B and C are somewhat blue-shifted in comparison to the fluid solution results. The higher energy emission feature A is still observed from the 4-Phpy complex as a shoulder at low temperature, but in the py complex it is apparently hidden by the neighboring band B, and we were also unable to resolve it by lifetime measurements. Emission lifetimes recorded at 80 K now are all on the microsecond time scale, and each band has a unique value (see Table I). No emission was observed on excitation of $CpRe(CO)_3$ in an EPA glass at 80 K.

Excitation spectra have been recorded while monitoring the emission at each of the maxima A, B, and C; results obtained for $CpRe(CO)_2(4\text{-Phpy})$ and $CpRe(CO)_2(pip)$ in 293 K benzene are shown in Figure 3. Absorption spectra of these complexes are included for comparison purposes. Excitation spectra obtained while monitoring the emission from either of the low-energy emission bands B and C of $CpRe(CO)_2(4\text{-Phpy})$ exhibit three maxima, the low-energy region showing fairly good congruence with the intense absorption band envelope. These spectra were essentially invariant on monitoring the emission at wavelengths between the maxima of bands B and C. On the other hand, monitoring at the high-energy emission band A (440 nm) of

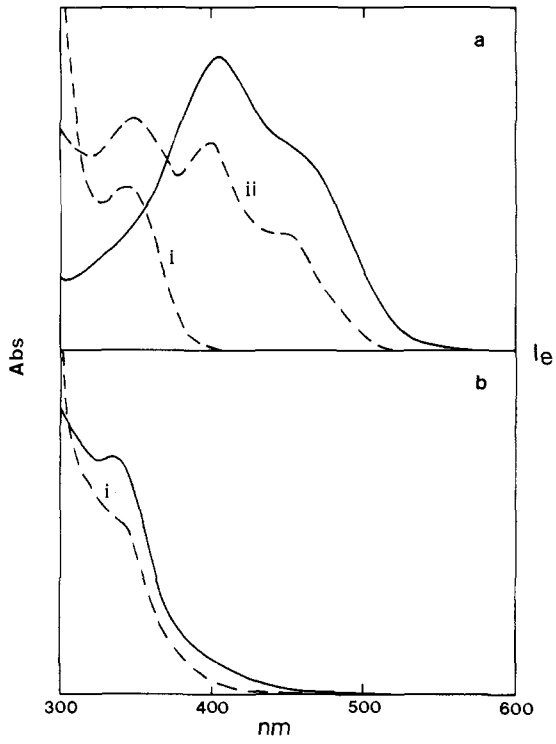

Figure 3. Electronic absorption (—) and excitation (--) spectra of (a) $CpRe(CO)_2$(4-Phpy) and (b) $CpRe(CO)_2$(pip) in deoxygenated benzene at 293 K. Excitation spectra are corrected for variations in instrumental response as a function of wavelength; emission monitored at 440 nm (i) and 600 nm (ii).

$CpRe(CO)_2$(4-Phpy) results in a single excitation maxima at 346 nm (see Figure 3). Similar results were also obtained from $CpRe(CO)_2$(py) (see Table I). Significantly, the $CpRe(CO)_2$(pip) complex also exhibits an excitation maximum at 344 nm which is congruent with its lowest lying absorption band.

Excitation wavelength variations on the emission spectra were investigated for all of the complexes. The emission maxima themselves were found to be independent of excitation wavelength, but the relative intensities of the three emission bands are affected. The ratio of band A with respect to band B for the $CpRe(CO)_2L$ (L = py and 4-Phpy) complexes in 293 K solution is substantially increased on exciting at shorter wavelengths; representative spectra are illustrated in Figure 4 for the 4-Phpy complex. Contrastingly, the ratio of the intensities of the two lower lying emission bands B and C remains constant on excitation at any wavelength throughout the broad absorption band envelope. Similar observations were made for the analogous $CpRe(CO)_2$(py) complex. In addition, the emission spectrum of $CpRe(CO)_2$(pip), which exhibits a single band, is not shifted on varying the excitation wavelength through the 305–340-nm region. In EPA glasses at 80 K substantial excitation wavelength effects are observable on the intensities of all the emission maxima of $CpRe(CO)_2L$ (L = py and 4-Phpy); representative spectra are shown in Figure 5 for $CpRe(CO)_2$(4-Phpy). When the shorter excitation wavelengths are used, the higher energy emission bands A and B become more prominent, although, again, their energy positions are not changed.

Figure 6 illustrates the effects that are observed on the emission spectrum of $CpRe(CO)_2$(4-Phpy) in deoxygenated toluene as the solution temperature is lowered from 293 to 213 K. When the solution is cooled, there are considerable changes in the low-energy region of the emission spectrum with band B gaining intensity significantly and a concomitant diminishing of band C. An isoemissive point at 586 nm is retained in the spectra throughout these temperature changes. In comparison, the intensity of band A is relatively unaltered on lowering the fluid solution temperature from 293 to 210 K. The total quantum yield and emission lifetime for bands B and C of $CpRe(CO)_2$(4-Phpy) in toluene at 293 K were determined to be 2.1×10^{-4} and 1.66 μs, respectively. From gaussian deconvolutions of the spectra represented in Figure 6

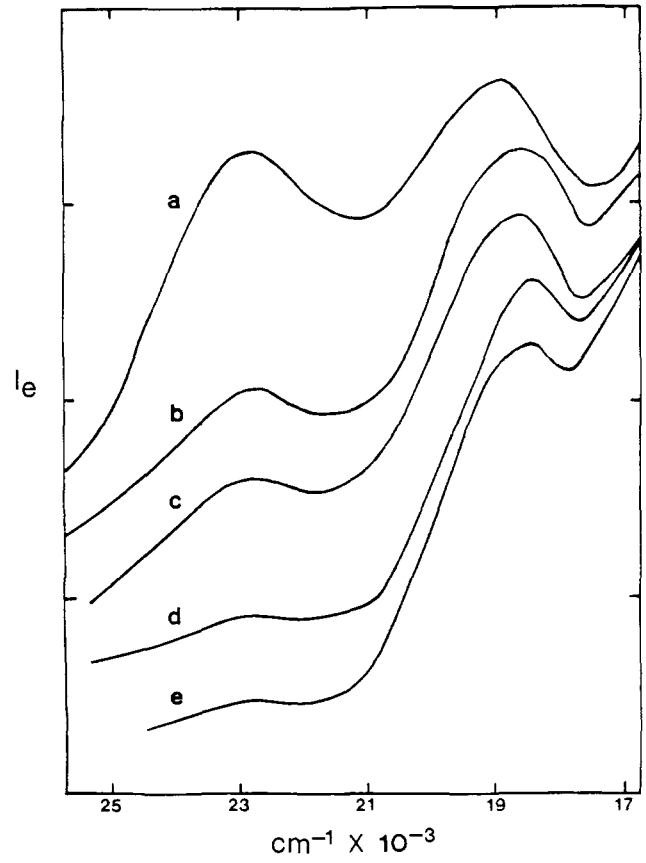

Figure 4. Emission spectra observed from $CpRe(CO)_2$(4-Phpy) in deoxygenated benzene at 293 K following excitation at (a) 305, (b) 310, (c) 320, (d) 330, and (e) 340 nm. Individual spectra are normalized following correction for wavelength variations in detector response.

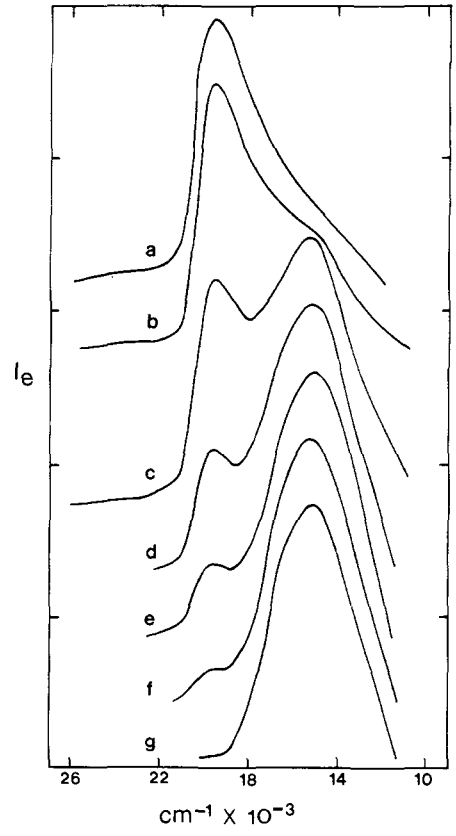

Figure 5. Emission spectra observed from $CpRe(CO)_2$(4-Phpy) in EPA at 80 K following excitation at (a) 300, (b) 320, (c) 330, (d) 340, (e) 350, (f) 360, and (g) 380 nm. Individual spectra are normalized following correction for wavelength variations in detector response.

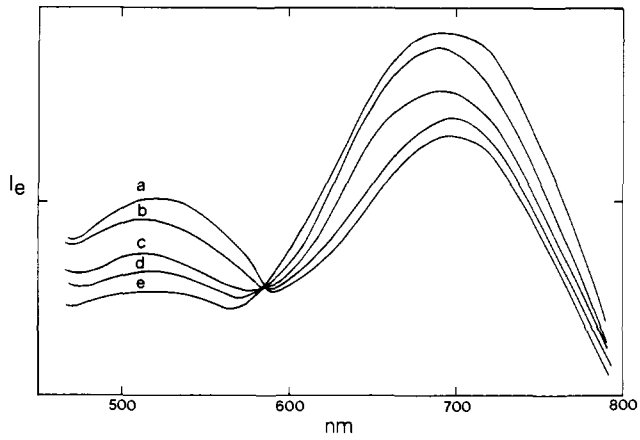

Figure 6. Temperature dependence of emission spectra from $CpRe(CO)_2$(4-Phpy) in deoxygenated toluene following excitation at 370 nm; temperatures are (a) 213, (b) 233, (c) 253, (d) 273, and (e) 293 K. Spectra are corrected for wavelength variations in detector response.

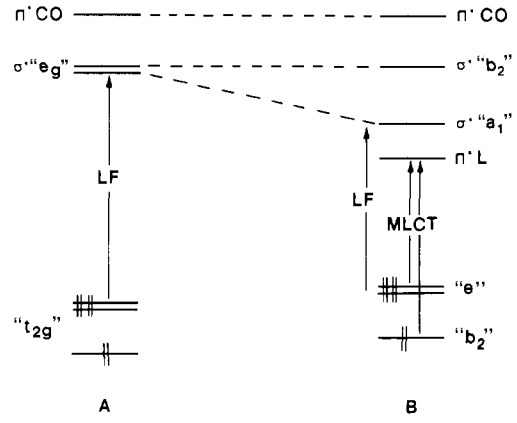

Figure 7. Molecular orbital scheme for (a) pseudo-O_h $CpRe(CO)_3$ and (b) pseudo-C_{4v} $CpRe(CO)_2L$ (L = py or substituted py) complexes. For clarity only the lowest lying LF and MLCT transitions are illustrated.

the relative quantum yield ratios of band C/band B at the stated temperatures are 3.54 (293 K), 2.00 (273 K), 1.50 (253 K), 0.90 (233 K), and 0.71 (213 K).

Discussion

Excited-State Assignments. Previously, Giordano and Wrighton have studied the relationship between electronic structure and photosubstitution reactivity for a series of $CpM(CO)_2L$ (M = Mn, Re; L = CO or a N-donor ligand) complexes.[12] In their interpretation the $CpM(CO)_3$ species were viewed in a "pseudo-O_h" symmetry and the $CpM(CO)_2L$ complexes as being of a "perturbed-C_{4v}" symmetry. A molecular orbital description based on these symmetry approximations is illustrated in Figure 7. In this simple MO model the lowest energy transitions in $CpRe(CO)_3$ are of ligand field (LF) character, and in $CpRe(CO)_2L$ (L = py or 4-Phpy) they are of metal-to-ligand charge-transfer (MLCT) character; the latter transitions originate from orbitals of "b_2" and "e" symmetries following the degeneracy removal of the filled "t_{2g}" type orbitals. Although this MO description is a gross approximation, it does prove useful in rationalizing the obtained electronic absorption and photophysical data. For convenience, the two low-lying $Re(d\pi) \rightarrow (\pi^*)L$ transitions in the $CpRe(CO)_2L$ (L = py and 4-Phpy) compounds will be referred hereafter as the MLCT(b_2) and MLCT(e) states.

a. Electronic Absorption Spectra. Our absorption spectral observations are entirely in accordance with the proposed electronic structure model. Absorption spectra of $CpRe(CO)_2L$ (L = py and 4-Phpy) are dominated by two intense MLCT features in the visible region; these bands are assigned to the MLCT(b_2) and MLCT(e) states, the latter transition being at lowest energy and observed as a shoulder in the absorption spectrum (see Figure 1). Noticeably, both transitions exhibit solvent and substituent dependencies, characteristic of those observed from MLCT spectra of other metal carbonyl systems.[1c,d] Moreover, the MLCT bands are temperature/environment sensitive, shifting to higher energy when the solution is cooled to 80 K and forming a frozen glass (see Figure 1). This "rigidochromic effect" is one recognized for other organometallic species and is understood to be a type of a solvent environment effect deriving from the reorientation of the solvent dipoles around the metal complex as the medium becomes rigid.[1d,18]

Contrastingly, the $CpRe(CO)_2$(pip) complex possesses no $Re(d\pi) \rightarrow (\pi^*)L$ MLCT transitions, and the lowest absorption band at ~340 nm (see Table I and Figure 3) is attributed to the lowest lying "e" $\rightarrow$ "a_1"(σ^*) LF transition (see Figure 7). In accordance with this assignment the absorption spectrum of the $CpRe(CO)_2$(pip) complex is not significantly temperature dependent. The lowest lying LF level is anticipated to be about the same energy in the py and 4-Phpy derivatives and it is observed as a weak high energy shoulder on the MLCT absorption band envelope of the $CpRe(CO)_2$(4-Phpy) complex (see Figure 1). In the analogous $CpRe(CO)_2$(py) species the corresponding lowest lying LF absorption band is completely hidden by the intense neighboring MLCT transitions which lie at somewhat higher energies (see Table I).

b. Luminescence Data. Each of the $CpRe(CO)_2$(py) and $CpRe(CO)_2$(4-Phpy) complexes display three distinct emission maxima in room-temperature benzene solution (see Figure 2 and Table I). The two lowest lying emissions (bands B and C) are noted to be both solvent and substituent dependent and are, therefore, associated with the MLCT(b_2) and MLCT(e) levels. These emission bands are presumed to be from the "triplet" excited states, to the extent that spin is a "good" quantum number in these metal complexes.[19] A third rather weak emission feature (band A) is observed at higher energy in the $CpRe(CO)_2L$ (L = py and 4-Phpy) complexes; this band exhibits relatively little solvent and substituent dependencies and, consequently, is assigned to the lowest lying triplet LF state. Importantly, the $CpRe(CO)_2$(pip) complex also yields this ^{3}LF emission feature (see Figure 2).

Emission spectra of these $CpRe(CO)_2L$ complexes undergo significant changes when the solution is cooled to 80 K, and these changes are consistent with the ^{3}MLCT and ^{3}LF assignments. Both ^{3}MLCT emission bands blue shift substantially when the solution is cooled to a frozen glass, whereas the ^{3}LF features are relatively unaltered (see Table I). Previously, it has been shown that MLCT emission bands are especially affected when the solution changes from a dynamic solution to a rigid solution environment; this phenomenon has been termed "luminescence rigidochromism"[18a,20] and has been observed for a number of other substituted metal carbonyl complexes.[1d,4d,18a,b] It is analogous to the effect noted above in the absorption spectra.

Emission lifetimes obtained from the $CpRe(CO)_2L$ complexes at 80 and 293 K (see Table I) also support the ^{3}MLCT and ^{3}LF assignments. In 293 K solution the $CpRe(CO)_2$(4-Phpy) complex exhibits a very short decay ($\tau_e < 0.5$ ns) from the high energy band A which is attributed to the ^{3}LF emission. The $CpRe(CO)_2$(pip) also yields a short emission lifetime ($\tau_e = 0.5$ ns). In contrast, the emission decays of bands B and C for either $CpRe(CO)_2$(py) or $CpRe(CO)_2$(4-Phpy) are much longer (τ_e = 1–5 μs) and are associated with the ^{3}MLCT levels. Significantly, in either complex at any fixed temperature between 210 and 293 K the solution lifetimes are identical throughout bands B or C, suggesting that the ^{3}MLCT(b_2) and ^{3}MLCT(e) states are rapidly interconverting and, thus, thermally equilibrated in fluid solution. At 80 K, however, the emission lifetimes observed from each of the emission bands are unique (see Table I), implying that the

(18) (a) Wrighton, M.; Morse, D. L. *J. Am. Chem. Soc.* **1974**, *96*, 998. (b) Salman, O. A.; Drickamer, H. G. *J. Chem. Phys.* **1982**, *77*, 3337. (c) Zulu, M. M.; Lees, A. J. *Inorg. Chem.* **1988**, *27*, 3325.

(19) Spin-orbit coupling in these heavy metal complexes precludes describing them as "pure" triplets. See ref 1d for further discussion of this subject.

(20) Giordano, P. J.; Fredericks, S. M.; Wrighton, M. S.; Morse, D. L. *J. Am. Chem. Soc.* **1978**, *100*, 2257.

^{3}MLCT manifold is not in thermal equilibrium in a low-temperature frozen glass (vide infra).

Observations of ^{3}LF emissions at room temperature are unusual for metal carbonyl complexes,[1d] as ^{3}LF states are normally expected to be extremely short-lived and difficult to experimentally observe. This is because ^{1,3}LF levels are typically highly reactive, and their emission routes suffer from rapidly competing nonradiative processes. Recently, though, there have been other reports of ^{3}LF emission from $XRe(CO)_4L$ (X = Cl, I; L = a P or N donor ligand)[21] and $M(CO)_4(\alpha,\alpha'$-diimine) (M = Mo, W; α,α'-diimine = a substituted phen ligand)[22] complexes under room-temperature fluid conditions, and these emission decays are also rapid. Noticeably, emission was not observable from the parent $CpRe(CO)_3$ complex either in solution at 293 K or in frozen EPA at 80 K, despite a lowest lying ^{1,3}LF assignment like the emissive $CpRe(CO)_2$(pip) complex. However, in the case of $CpRe(CO)_3$ the lowest energy ^{1,3}LF levels lie in close proximity to the $Re(d\pi) \rightarrow (\pi^*)CO$ states (see Figure 7), which in turn may mix with the ^{1,3}LF levels and quench the emission. A similar rationale has been used to account for the absence of ^{3}LF emission from $XRe(CO)_5$ (X = Cl, I) compounds in EPA glassy solutions at 80 K.[21b]

Excitation spectra recorded from $CpRe(CO)_2$(4-Phpy) in 293 K solution can be explained with the use of the triply emitting excited-state model. When the emission is monitored at wavelengths corresponding to either of the MLCT emission maxima (bands B and C), the excitation spectra were noted to be essentially the same, exhibiting features centered at 346, 402, and 450 nm (see Figure 3a). The two lowest energy features are congruent with the MLCT absorption band envelope and, therefore, are assigned to the ^{1,3}MLCT(b_2) and ^{1,3}MLCT(e) levels. Furthermore, the invariance of the excitation spectrum on monitoring at the wavelengths of emission bands B and C confirms the thermally equilibrated nature of these ^{3}MLCT levels. The upper excitation band, observed at 346 nm, is associated with the ^{1,3}LF manifold which efficiently nonradiatively populates the emitting ^{3}MLCT states. On the other hand, when the emission is monitored at a wavelength corresponding to the ^{3}LF emission (band A), the excitation spectrum displays a single feature at 346 nm that is attributed to direct radiative deactivation of the ^{3}LF level. This result further indicates that the ^{3}LF emission is not equilibrated with the lower ^{3}MLCT states. Consistent with this interpretation the $CpRe(CO)_2$(pip) complex gives rise to a single excitation band centered at 344 nm, and this is associated with the ^{3}LF state. Excitation spectra from $CpRe(CO)_2$(py) are very similar to those displayed by $CpRe(CO)_2$(4-Phpy), and accordingly the MLCT excitation bands lie at somewhat higher energies (see Table I).

Emission spectra recorded at various excitation wavelengths further illustrate the nature of the $CpRe(CO)_2L$ photophysical system. In 293 K solution the lowest energy emission bands B and C of both the $CpRe(CO)_2L$ (L = py, 4-Phpy) complexes exhibit no discernible variation when the exciting wavelength is moved within the broad MLCT absorption band envelope, reinforcing the notion of the equilibrium between the participating ^{3}MLCT(b_2) and ^{3}MLCT(e) levels. In contrast, the ratio of the intensity of emission band A with respect to that of emission band B is greatly affected when the excitation wavelength is changed (see Figure 4); this result provides additional evidence that the emission arising from the ^{3}LF level is independent of the ^{3}MLCT system. Moreover, the absence of an excitation wavelength dependence on the emission spectrum of $CpRe(CO)_2$(pip) supports the single emitting ^{3}LF state model proposed for this complex. At 80 K, all three emission bands of $CpRe(CO)_2L$ (L = py, 4-Phpy) apparently originate from excited states emitting independently as there is a strong dependence on the excitation wavelength employed (see Figure 5). It is concluded that in a frozen EPA glass at 80 K the thermal equilibrium that existed between the ^{3}MLCT(b_2) and ^{3}MLCT(e) levels is now lost. Similar excitation wavelength dependence on low-temperature emission spectra has been observed for other metal carbonyl systems,[1d] including isoelectronic *fac*-$[SRe(CO)_3(phen)]^+$ (S = CH_3CN, PhCN, py, pip) and *fac*-$[XRe(CO)_3L]$ (X = Cl, Br, I; L = py or a substituted py) complexes that display multiple emission from $Re \rightarrow \pi^*(L)$ and IL levels.[20,23]

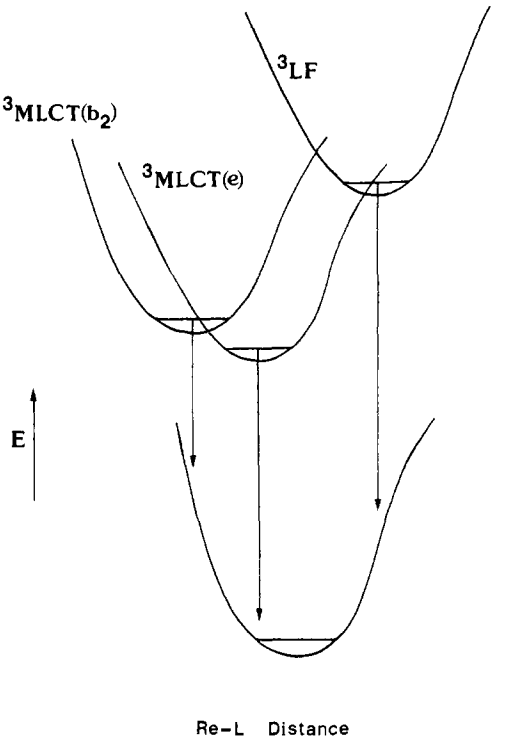

Figure 8. Schematic representation of the radiative process involving the ^{3}LF, ^{3}MLCT(b_2), and ^{3}MLCT(e) excited states of $CpRe(CO)_2L$ (L = py or substituted py). For clarity, internal conversions and other nonradiative processes are omitted.

Valuable information on the energy order of the ^{3}MLCT(b_2) and ^{3}MLCT(e) emitting levels is obtained from the temperature dependence of the $CpRe(CO)_2$(4-Phpy) emission spectra. When the solution temperature is lowered from 293 to 210 K the ^{3}MLCT emission feature appearing at higher energy (band B) gains intensity appreciably, and the intensity of the lower energy emission (band C) is reduced (see Figure 6). This behavior is exactly the opposite to that one would expect for a thermally equilibrated system in which the ^{3}MLCT(e) state is assigned as band C. The apparent contradiction is reasoned on a potential-energy diagram (see Figure 8) that qualitatively represents the equilibrium geometries and energies of the excited states relative to the ground state. In this description the higher energy ^{3}MLCT(b_2) level is shown to be more distorted from the ground-state equilibrium geometry than the ^{3}MLCT(e) level, thus, the ^{3}MLCT(b_2) state gives rise to emission band C at lowest energy. We have chosen to express the nuclear coordinate as the average equilibrium geometry of the Re–L bond because on MLCT excitation the metal is formally oxidized and the ligand is reduced. Moreover, the ^{3}MLCT states are depicted to undergo a compression of the Re–L bond concordant with the induced dipole that is produced and the reduced photosubstitutional chemistry of ^{3}MLCT excited states.[1c,d] On the other hand, the ^{3}LF state is shown to undergo an elongation of the Re–L bond because of the high photoreactivity associated with this level.[12] In this connection, time-dependent theoretical analyses of emission and preresonance Raman spectra of $W(CO)_5L$ (L = a N donor ligand) complexes have indicated that on LF excitation the most significant excited-state distortion that takes place is a lengthening of the W–N bond.[24] Similar

(21) (a) Glezen, M. M.; Lees, A. J. *J. Chem. Soc., Chem. Commun.* **1987**, 1752. (b) Glezen, M. M.; Lees, A. J. *J. Am. Chem. Soc.* **1988**, *110*, 3892.

(22) (a) Servaas, P. C.; van Dijk, H. K.; Snoeck, T. L.; Stufkens, D. J.; Oskam, A. *Inorg. Chem.* **1985**, *24*, 4494. (b) Manuta, D. M.; Lees, A. J. *Inorg. Chem.* **1986**, *25*, 1354. (c) Rawlins, K. A.; Lees, A. J. *Inorg. Chem.* **1989**, *28*, 2154.

(23) (a) Fredericks, S. M.; Luong, J. C.; Wrighton, M. S. *J. Am. Chem. Soc.* **1979**, *101*, 7415. (b) Giordano, P. J.; Wrighton, M. S. *J. Am. Chem. Soc.* **1979**, *101*, 2888.

potential-energy representations involving compression of Re–L bonds in ^{3}MLCT excited states have been proposed for *fac*-[XRe(CO)$_3$L$_2$] (X = Cl, Br, I; L = 4,4′-bpy, 4-Phpy) complexes,[23b] although it should be noted that a scheme involving elongation of the Re–L bonds could equally account for our luminescence data.

Excited-State Dynamics. In the above excited-state assignments a model of an emitting ^{3}LF state lying above two emissive ^{3}MLCT(b_2) and ^{3}MLCT(e) states has been described. The ^{3}MLCT excited state manifold is understood to be thermally equilibrated in fluid solution but not in a frozen glassy solution. The ^{3}LF state gives rise to an independent (nonequilibrated) and relatively rapid radiative pathway to the ground state. At this stage we will address possible reasons leading to the nonequilibrium behavior observed at both room and low temperature and further explore the rates of the excited-state deactivation mechanisms.

a. Nonequilibrated Excited States at 80 K. Nonequilibrating photophysical systems in low-temperature glasses have been discussed in the literature in considerable detail,[3] and some generalizations concerning them can be made. Of course, it is important to recognize that adequate experimental care must have first been taken to rule out the trivial examples of multiple emission, such as that arising from the presence of impurities or photoproduced emitting species in the glass environment, and these cases are not further discussed here.

Multiple nonequilibrated emission can occur due to a type of preferential solvation in the microenvironment, where two (or more) emissions are observed resulting from differing solvent environments. Also, nonequilibrated emission can arise from mixed ligand systems where each emission is a localized single ring emission. This particular type of multiple luminescence has been observed from a number of complexes, including Rh(bpy)$_2$(phen),$^{3+}$ Ru(phen)$_2$(bpy),$^{3+}$ and Ir(phen)Cl$_2$L$^+$ (L = 5,6-Me$_2$-phen or 4,7-Me$_2$-phen).[3a,25] The participating states are thought to behave as different species with limited interconversion between them. A third type of multiple luminescence is distinct orbital emission. This is similar in experimental observation to a single ring emission and is the most common type of multiple emission at low temperature.[3a,g,20,23,26] Here, because of differing orbital geometries, there is very little overlap between the states and most probably also significant microenviornmental differences. Therefore, the interconversion rates between the levels are slow with respect to the radiative and nonradiative deactivation pathways; this can occur even when the two participating states are at about the same energy.

Since in our case there are two quite different orbital transitions associated with the MLCT and LF excited states, it seems most likely that these nonequilibrated emissions fall into the category of a distinct orbital emitter. As noted earlier, there are other known examples of multiple emissions involving a ^{3}IL (or ^{3}LF) state and a ^{3}MLCT state which can be assigned to distinct orbital emitters. It is, though, much rarer to find examples where two ^{3}MLCT states do not interconvert readily as we have observed at low temperature. However, if one considers that the ^{3}MLCT(b_2) and ^{3}MLCT(e) excited states are not only of different orbital origin but are also thought to be of a very different geometry (vide supra), it is reasonable to expect them to be nonequilibrated in a frozen glassy solution. In this regard, recent luminescence and resonance Raman spectra obtained from W(CO)$_4$(α,α′-diimine) and binuclear (OC)$_5$W-L-W(CO)$_5$ systems have illustrated that their proximate MLCT excited states are very different not only in their orbital origin but also in their geometry and solvation.[18c,22,27] Thus, the slow interconversion between the two ^{3}MLCT levels in the CpRe(CO)$_2$L system at 80 K is attributed primarily to the large differences in the distortion of the participating charge-transfer excited states.

b. Nonequilibrated Excited States at 293 K. Nonequilibrating photophysical systems at room temperature are extremely rare and have been limited to only a few literature examples. recently, two rapid emission decays have been associated with the LF luminescence of RhL$_5$X^{2+} (L = NH$_3$, ND$_3$; X = Cl, Br) in aqueous solution at 298 K.[6b] The longer lived decay was on the order of 1–13 ns, and a very rapid component was determined with a 50–250 ps lifetime. This nonequilibrated behavior was rationalized on the basis of a singlet–triplet scheme and is supported by measurements at 277 K indicating an increase in the triplet state lifetime but essentially no change in the singlet state lifetime. Intersystem crossing rates between these singlet and triplet levels have been estimated to be on the order of $1/\tau_f$ (τ_f = fluorescence lifetime), yielding a lower limit of 10^9 s^{-1}. Nonequilibrium behavior has also been observed from several Cr(III) systems in aqueous solutions, and similar types of singlet–triplet models have been adopted.[28] However, a singlet–triplet model would not appear to adequately account for our room-temperature multiple luminescence data as the ^{3}LF and ^{3}MLCT lifetimes are each temperature dependent and, thus, thought to be predominantly triplet-centered.

We are aware of one example of nonequilibrated multiple luminescence from a metal complex which does not incorporate a singlet–triplet model. This concerns the Ru(NH$_3$)$_5$(DMABN)$^{2+}$ (DMABN = (dimethylamino)benzonitrile) system which luminesces from ligand-localized levels, and the multiple emission has been associated with the concept of twisted internal charge-transfer (TICT) states.[29] The literature on TICT states is extensive, and it primarily deals with organic compounds.[30] However, the data obtained for the CpRe(CO)$_2$(4-Phpy) complex do not appear to fit this TICT model because of two reasons. First, the free 4-Phpy ligand itself should exhibit similar TICT behavior in solution, and this was not observed under our experimental conditions. Second, typical TICT lifetimes observed are on a picosecond–nanosecond time scale, much faster than our nanosecond–microsecond lifetimes. Also, the py complex, where the ligand is not able to undergo this type of twist, shows similar emission properties. Therefore, the CpRe(CO)$_2$L system appears to be the first instance of nonequilibrated emission arising from two triplet levels of an organometallic complex under fluid solution conditions. The key to understanding the nonequilibration behavior seems to lie in the system's excited-state deactivation rate constants.

c. Photophysical Parameters. Radiative decay rate constants (k_r) can be obtained for the CpRe(CO)$_2$L system following a kinetic analysis. In the case of CpRe(CO)$_2$(pip), the determination is relatively straightforward as the ^{3}LF emission involves only the single lowest energy excited state. From the quantum yield (ϕ_e) and lifetime (τ_e) data of Table I and $k_r = \phi_e/\tau_e$, a k_r value of 2.6 $\times$ 10^6 s^{-1} is calculated. Notably, this value is several orders of magnitude greater than estimates of k_r for ^{3}MLCT emissions of other metal carbonyl complexes,[1d,18c,31] and it is commensurate with those for ^{3}LF decay of the XRe(CO)$_4$L system.[21] In this connection, the UV–vis spectra obtained clearly indicate that the integrated absorption intensities of the LF levels are much less than those of the MLCT levels and, thus, the radiative lifetime of the ^{3}LF state ought, in theory, to be longer than the ^{3}MLCT emission. However, the k_r value here is derived from experimental data, whereas its theoretical value fails to take into account competing radiationless processes. Consequently, a rapid k_r value for ^{3}LF emission is not unreasonable from an excited state that is characterized by efficient photodissociation pathways competing with the radiative mechanism.[12] The presence of overlapping MLCT absorption bands for the CpRe(CO)$_2$(4-Phpy) complex makes a ^{3}LF decay estimate unreliable, but it is assumed that the

(24) Tutt, L.; Zink, J. I. *J. Am. Chem. Soc.* **1986**, *108*, 5830.
(25) (a) Halper, W.; DeArmond, M. K. *J. Lumin.* **1972**, *5*, 225. (b) Watts, R. J.; Brown, M. J.; Griffith, B. G.; Harrington, J. S. *J. Am. Chem. Soc.* **1975**, *97*, 6029.
(26) Watts, R. J.; White, T. P.; Griffith, B. G. *J. Am. Chem. Soc.* **1975**, *97*, 6914.
(27) (a) Daamen, H.; Stufkens, D. J.; Oskam, A. *Inorg. Chim. Acta* **1980**, *19*, 3519.
(28) Kane-Maguire, N. A. P.; Langford, C. H. *J. Chem. Soc., Chem. Commun.* **1971**, 895.
(29) Sowinska, M.; Launay, J.-P.; Mugnier, J.; Pouget, J.; Valeur, B. *J. Photochem.* **1987**, *37*, 69.
(30) Rettig, W. *Angew. Chem., Int. Ed. Engl.* **1986**, *25*, 971.
(31) Zulu, M. M.; Lees, A. J. *Inorg. Chem.* **1988**, *27*, 1139.

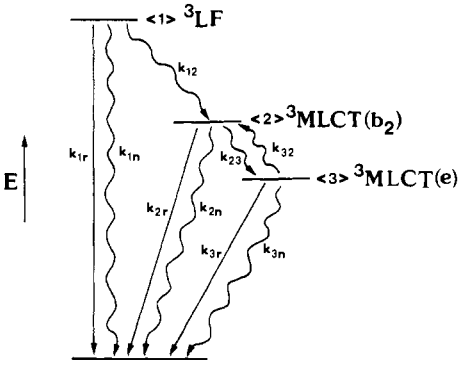

Figure 9. Photophysical deactivation scheme for the lowest lying states of CpRe(CO)$_2$L (L = py or substituted py) in room-temperature solution. Vertical and wavy lines represent radiative and radiationless processes, respectively.

radiative decay rate would be at least 2.6×10^6 s^{-1} as the measured lifetime (τ_e <0.5 ns) is below the capability of our instrumentation. Actually, the ^{3}LF radiative rate should be much greater for CpRe(CO)$_2$(4-Phpy) than for CpRe(CO)$_2$(pip) because of additional nonradiative routes to the ^{3}MLCT manifold lying below. A key feature of this photophysical system is, therefore, the presence of a ^{3}LF state which rapidly deactivates radiatively, thereby providing a radiative route that is competitive with all other nonradiative processes, including bond dissociation and internal conversions to lower lying ^{3}MLCT levels.

Further analysis of the emission temperature dependence data (see Figure 6) yields the radiative rates from the thermally equilibrated ^{3}MLCT(b_2) and ^{3}MLCT(e) states. Figure 9 depicts the photophysical scheme for the CpRe(CO)$_2$L system, showing the distorted ^{3}MLCT(b_2) state at higher energy than the ^{3}MLCT(e) state. The first deactivation model considered is the kinetic limit, previously discussed in detail by Parker,[32] where the emission from the upper ^{3}MLCT(b_2) emitting level ⟨2⟩ is associated with both prompt and delayed emission processes. In this model it is assumed that ^{3}MLCT(b_2) reaches a steady-state concentration that is not significantly affected by the reverse population from ^{3}MLCT(e). Consequently, delayed emission efficiency ($\phi_{delayed}$) from ^{3}MLCT(b_2) is represented by eq 1 and 2.[4b,5,32] Here, ϕ_2 is the emission efficiency of prompt emission,

$$\phi_{delayed} = \frac{k_{2r}}{k_{23} + k_{2r} + k_{2n}} \frac{k_{23}}{k_{23} + k_{2r} + k_{2n}} \frac{k_{32}}{k_{32} + k_{3r} + k_{3n}} \quad (1)$$

$$\phi_{delayed} = \phi_2\phi_{23}\phi_{32} \quad (2)$$

ϕ_{23} is the efficiency by which the ^{3}MLCT(b_2) state converts to the ^{3}MLCT(e) state, and ϕ_{32} is the efficiency of back population. This deactivation model does not fit with the observed emission data for two reasons. First, if one assumes that vibrational relaxation is faster than k_{23}, the delayed fluorescence model predicts mostly prompt emission, i.e., emission appearing within the lifetime of the ^{3}MLCT(b_2) state. This is not reflected by our emission lifetime data which indicates that band C is dominated by a microsecond decay and not a short-lived component. Second, delayed fluorescence or thermally activated emission typically exhibit a much greater temperature dependence than that observed here.

Instead, the obtained emission data are better accounted for by considering an equilibrium limit.[4b,5] The primary premise of this model is that the k_{23} and k_{32} rates are rapid compared to the other deactivation processes from the ^{3}MLCT states, i.e., $k_{23} \gg k_{2r} + k_{2n}$ and $k_{32} \gg k_{3r} + k_{3n}$. At the equilibrium limit the steady-state concentrations of the two emitting ^{3}MLCT levels are described by a Boltzmann population. Firstly, the equilibrium constant and the common emission lifetime of the two states are defined by eq 3 and 4, respectively.

(32) Parker, C. A. *Adv. Photochem.* **1964**, *2*, 305.

$$K = [^3\text{MLCT}(b_2)]/[^3\text{MLCT}(e)] = k_{32}/k_{23} \quad (3)$$

$$\tau_e = \frac{1 + K}{k_{3r} + k_{3n} + (k_{2r} + k_{2n})K} \quad (4)$$

The quantum yields of the ^{3}MLCT(b_2) and ^{3}MLCT(e) states are expressed by eq 5 and 6, respectively.

$$\phi_2 = \frac{k_{2r}K}{k_{3r} + k_{3n} + (k_{2r} + k_{2n})K} \quad (5)$$

$$\phi_3 = \frac{k_{3r}}{k_{3r} + k_{3n} + (k_{2r} + k_{2n})K} \quad (6)$$

Thus,

$$\phi_3/\tau_e = k_{3r}/(1 + K) \quad (7)$$

where $1/(1 + K)$ is temperature dependent and equal to the interconversion quantum yield ϕ_{23} between the two equilibrated ^{3}MLCT states, and where $\phi_{23} = k_{23}/(k_{2r} + k_{2n} + k_{23})$. Expressing K in terms of a Boltzmann distribution between these levels gives

$$K = \frac{g[\text{MLCT}(b_2)]}{g[\text{MLCT}(e)]} \exp(-\Delta E/k_B T) \quad (8)$$

where g[MLCT(b_2)] and g[MLCT(e)] represent the Boltzmann degeneracy factors of the ^{3}MLCT states, ΔE is the energy gap between these levels, k_B is the Boltzmann constant, and T is temperature. Substituting eq 8 into eq 7 yields

$$\frac{\phi_3}{\tau_e} = \frac{k_{3r}}{1 + \{g[\text{MLCT}(b_2)]/g[\text{MLCT}(e)]\} \exp(-\Delta E/k_B T)} \quad (9)$$

If $\Delta E > 1000$ cm^{-1}, then eq 9 reduces to $\phi_{3r} = k_{3r}\tau_e$, and the two participating states are no longer regarded to be thermally equilibrated. Dividing eq 5 by eq 6 and rearrangings yields

$$K = \frac{\phi_2 k_{3r}}{\phi_3 k_{2r}} \quad (10)$$

and substitution into eq 8 gives

$$\frac{\phi_2}{\phi_3} = \frac{g[\text{MLCT}(b_2)]k_{2r}}{g[\text{MLCT}(e)]k_{3r}} \exp(-\Delta E/k_B T) \quad (11)$$

Subsequently, ΔE is determined from the quantum yield ratios in Figure 6 by plotting $\ln(\phi_2/\phi_3)$ vs $1/T$. A least-squares analysis of the data gives $\Delta E = 860(\pm 100)$ cm^{-1}, and a y-intercept = 5.34. Assuming the 3-fold degeneracy for both MLCT triplet levels then $k_{2r}/k_{3r} = 208$, and K is calculated by using eq 8 to be 1.46×10^{-2} at 293 K. Combining eqs 4–6 gives

$$\frac{\phi_{tot}}{\tau_e} = \frac{\phi_2 + \phi_3}{\tau_e} = \frac{k_{2r}K + k_{3r}}{1 + K} \quad (12)$$

Solving eq 12 yields $k_{2r} = 6.6 \times 10^3$ s^{-1} and $k_{3r} = 32$ s^{-1}, representing the radiative rates at 293 K from the ^{3}MLCT(b_2) and ^{3}MLCT(e) levels, respectively. These values are significantly lower than the above determined k_r value for the ^{3}LF emission and much more in line with the range anticipated for decays from electronically excited ^{3}MLCT states.[1d,18c,31]

Conclusions

A study of the temperature dependence and excitation wavelength dependence of the CpRe(CO)$_2$L (L = py or 4-Phpy) luminescence spectra and lifetimes leads to a photophysical model involving three emitting states. The two lowest energy emission features are attributed to arise from ^{3}MLCT excited levels that are separated by 860 cm^{-1}; these states are thermally equilibrated in fluid solution and are relatively long-lived, even at room temperature. The highest energy emission originates from a ^{3}LF excited state that rapidly deactivates and is not equilibrated with the ^{3}MLCT manifold. When the solution is cooled to 80 K and forms a frozen glass, the emission results obtained illustrate that all three ^{3}LF/^{3}MLCT excited states become nonequilibrated.

Additionally, the obtained photophysical data highlight the exceptionally long lifetimes that may be determined from ^{3}MLCT

states. Indeed, the possible role of these excited states in reaction chemistry, such as excited state electron transfer and intermolecular C-H bond activation mechanisms, remains to be fully explored.

Acknowledgment. We gratefully acknowledge the donors of the Petroleum Research Fund, administered by the American Chemical Society, and the Division of Chemical Sciences, Office of Basic Energy Sciences, Office of Energy Research, U.S. Department of Energy (Grant DE-FG02-89ER14039), for support of this research.

Registry No. $CpRe(CO)_2py$, 59423-85-7; $CpRe(CO)_2(4\text{-}Phpy)$, 60718-64-1; $CpRe(CO)_2pip$, 60718-65-2; $CpRe(CO)_3$, 12079-73-1.

Characterization of a Cobalt(II) Cyanide Complex inside Zeolite Y That Reversibly Binds Oxygen

Robert J. Taylor,[†] Russell S. Drago,*[,†] and James E. George[‡]

Contribution from the University of Florida, Department of Chemistry, Gainesville, Florida 32611, and DePauw University, Department of Chemistry, Greencastle, Indiana 46135. *Received December 22, 1988*

Abstract: We recently communicated the preparation of an anionic cobalt(II) cyanide complex inside zeolite Y that reversibly binds oxygen.[1] More complete characterization of this material is reported herein. Quantitative gas uptake measurements have shown this material to exhibit an enhanced adsorption of oxygen relative to its adsorption of argon. Enhanced oxygen adsorption was further demonstrated by comparison of zeolite Y containing an inert nickel cyanide complex to our active cobalt cyanide complex. This increase in oxygen uptake is due to the presence of an active cobalt complex. An equilibrium constant for the binding of oxygen to the active species was obtained from the oxygen and argon uptake isotherms. A similar result was obtained by measuring the intensity of the EPR signal for the $Co-O_2$ complex versus the oxygen pressure. The effect of the distribution coefficient for gas inside and outside the zeolite on the observed equilibrium constant is discussed. From the magnitude of the increased oxygen uptake, it is concluded that the active species is present in low concentration. This was confirmed by quantitative measurement of the EPR signal intensity for the oxygen adduct.

Cobalt complexes that reversibly bind dioxygen are available in a large variety of ligand systems.[2] The main drawback to the utilization of these materials in catalysis or oxygen enrichment from air arises from the fact that very few complexes bind oxygen in the solid state while in solution dimerization and irreversible oxidation of the complexes occur. Synthesizing these cobalt complexes inside the cage of a zeolite has the potential of eliminating these undesirable properties, and several zeolite-encapsulated metal complexes that reversibly bind dioxygen have been reported.[3] These compounds all involve neutral ligands, and though effective for separating oxygen from air, coordination of water as a sixth ligand or oxidation of the ligand limits their utility.[4] We have eliminated these problems by preparing an anionic cobalt cyanide complex within zeolite Y.[1] This complex is stable in the presence of water and can even be prepared in aqueous solutions. The cyanide ligand is very stable to oxidation and the zeolite prevents dimerization to form a μ-peroxo complex.

Experimental Section

Linde LZY-52 Na-Y zeolite was used as the starting material. It was slurried in 0.25 M NaCl solution, washed until no Cl^- was present in the filtrate, and dried at 100 °C under vacuum (10^{-3} Torr) prior to use. Unless otherwise stated, all reactions were carried out without any precautions to exclude air or atmospheric moisture.

Preparation of Cobalt Cyanide Containing Zeolites. Co-Y samples were prepared by exchanging Na^+ ions for Co^{2+} ions in an aqueous solution of $CoCl_2$ at 70 °C. After exchange, the solids were washed with water until no Cl^- was present in the filtrate. The resulting pink solids were dried at 150 °C under vacuum, yielding a deep blue solid. Ni-Y samples were prepared by using the same procedure. Co-Y(1) and Co-Y(2) contain 7.1 and 3.5 wt % cobalt, respectively. Ni-Y contains 3.4 wt % nickel.

Co(CN)-Y(1) and Co(CN)-Y(2) were prepared by reacting Co-Y(1) and Co-Y(2), respectively, with cyanide in a methanolic NaCN solution (CN:Co 10:1 minimum) at room temperature for 2-4 days. The resulting solids were washed with copious amounts of methanol and dried at 60 °C under vacuum. The resulting solids were gray-blue. The Ni(CN)-Y sample was prepared in the same way, resulting in a yellow solid after drying. Co(CN)-Y(3) was prepared from Co-Y(1) by using a much shorter reaction time and a minimum CN:Co ratio. Both Co(CN)-Y(1) and Co(CN)-Y(2) exhibit a single, sharp C-N stretching vibration at 2131 cm^{-1}. Co(CN)-Y(3) has an additional ν_{CN} at 2176 cm^{-1}. Ni(CN)-Y shows a single, sharp ν_{CN} at 2128 cm^{-1}.

Chelate treatment for removal of uncomplexed cobalt was carried out by stirring the samples with aqueous 0.1 M Na_4EDTA at 70 °C. The solids were then washed with water and dried at 60 °C under vacuum. The resulting solids are light yellow. This treatment also removes the ν_{CN} at 2176 cm^{-1} from Co(CN)-Y(3). The ν_{CN} at 2131 cm^{-1} remains unchanged.

Elemental Analysis. Cobalt concentrations were determined by ICP analysis of the dissolved zeolite. Typically, a 0.1-g sample of the zeolite was refluxed in 15 mL of 2 M HCl. Next, 10 mL of 6 M NaOH and 15 mL of 0.1 M Na_4EDTA were added, and the mixture was refluxed to completely dissolve the solid. The solution was then diluted to 100 mL and analyzed by using ICP. Analysis for nitrogen content was carried out by the Microanalysis Laboratory at the University of Florida. To ensure a constant weight during analysis for Co and N, the samples were allowed to equilibrate over H_2O in a closed chamber for several days prior to analysis. Water contents were calculated from the hydrogen content of the sample, and the reported weight percents are corrected back to dry samples.

[†] University of Florida.
[‡] DePauw University.

(1) Drago, R. S.; Bresinska, I.; George, J. E.; Balkus, Jr., K. J.; Taylor, R. J. *J. Am. Chem. Soc.* **1988**, *110*, 304.
(2) (a) Niederhoffer, E. C.; Timmons, J. H.; Martell, A. E. *Chem. Rev.* **1984**, *84*, 137. (b) Jones, R. D.; Summerville, D. A.; Basolo, F. *Chem. Rev.* **1979**, *79*, 139.
(3) (a) Howe, R. F.; Lunsford, J. H. *J. Phys. Chem.* **1975**, *79*, 1836. (b) Vansant, E. F.; Lunsford, J. H. *Adv. Chem. Ser.* **1973**, *121*, 441. (c) Howe, R. F.; Lunsford, J. H. *J. Am. Chem. Soc.* **1975**, *97*, 5156. (d) Mizumo, K.; Imamura, S.; Lunsford, J. H. *Inorg. Chem.* **1984**, *23*, 3510. (e) Herron, N. *Inorg. Chem.* **1986**, *25*, 4714.
(4) Imamura, S.; Lunsford, J. H. *Langmuir* **1985**, *1*, 326.

0002-7863/89/1511-6610$01.50/0